WILEY ONLINE LIBRARY
Early View publication on wileyonlinelibrary.com
(issue and page numbers not yet assigned;
citable using Digital Object Identifier – **DOI**)

Phys. Status Solidi RRL, 1–3 (2012) / **DOI** 10.1002/pssr.201206276

pss +++rapid research letters+++
www.pss-rapid.com

# On the mechanism of potential-induced degradation in crystalline silicon solar cells

**J. Bauer[*,1], V. Naumann[**,2], S. Großer[2], C. Hagendorf[2], M. Schütze[3], and O. Breitenstein[1]**

[1] Max Planck Institute of Microstructure Physics, Weinberg 2, 06120 Halle, Germany
[2] Fraunhofer Center for Silicon Photovoltaics CSP, Walter-Hülse-Str. 1, 06120 Halle, Germany
[3] Q-Cells SE, Sonnenallee 17–21, 06766 Bitterfeld-Wolfen, Germany

Received 25 June 2012, accepted 6 July 2012
Published online 10 July 2012

**Keywords** solar cells, crystalline silicon, potential induced degradation, sodium

[*] Corresponding author: e-mail jbauer@mpi-halle.mpg.de, Phone: +49 345 5582 761, Fax: +49 345 5511 223
[**] e-mail volker.naumann@csp.fraunhofer.de, Phone: +49 345 5589 119, Fax: +49 345 5589 101

Multicrystalline standard p-type silicon solar cells, which undergo a potential induced degradation, are investigated by different methods to reveal the cause of the degradation. Microscopic local ohmic shunts are detected by electron-beam-induced current measurements, which correlate with the sodium distribution in the nitride layer close to the Si surface imaged by time-of-flight secondary ion mass spectroscopy. The results are compatible with a model of the formation of a charge double layer on or in the nitride, which inverts the emitter.



Due to high voltages occurring in photovoltaic systems, solar modules may undergo so-called potential-induced degradation (PID) which may lead to significant performance losses [1]. These high voltages may cause leakage currents between the solar cells and the module frame through the front glass and encapsulation, being responsible for degradation effects [1–4].

Recently, PID was also observed at photovoltaic modules containing standard wafer based p-type Si solar cells subjected to negative bias with respect to the module frame [1, 3, 4]. It was also reported that the performance recovers upon positive biasing [1, 5] or by heating the module [1]. Elaborate PID investigation on cells and modules, e.g. in Refs. [4–6], revealed that the combination of soda lime glass, ethylene vinyl acetate (EVA) and the solar cell's anti reflective coating (ARC), which is the typical combination in commercial modules, is necessary for the formation of PID. Sodium originating from the soda lime glass plays a prominent role for the conductivity of the leakage current pathway [2]. Recently, the impact of sodium ions reaching the solar cell was investigated: Secondary ion mass spectroscopy (SIMS) measurements showed large concentrations of sodium within the ARC of PID affected cells [4, 7] and accumulation of those species on the ARC–silicon interface [8]. Precipitation of sodium at the surface of the cell and at defects in the ARC has also been reported [9]. However, the occurrence of PID in intentionally sodium free test setups was reported and the conclusion was made that PID is not correlated to a specific chemical species, e.g. sodium, but rather to ions of any species [3, 6]. PID of negatively biased p-type silicon solar cells is mainly characterized on a macroscopic level by a significant reduction of the parallel resistance $R_p$ (shunt) which decreases the performance of the cells [1, 3–9]. The destructive impact of PID on the p–n junction was also shown on a microscopic scale by electron-beam-induced current (EBIC) measurements [8]. Although the transport of metal ions to the cell surface during PID seems to be well established, the mechanism leading to a low $R_p$ of the solar cells is not clear yet. Our investigations focus on the root cause of PID related $R_p$ reduction and the role that ions play in the mechanism, starting from macroscopic level going down to microscopic investigations. Based on these observations we present a hypothesis on the mechanism of PID.

For the investigations a standard industrial screen printed, Al-back alloyed multicrystalline (mc) p-type Si solar cell was manufactured using a cell process, which results in cells prone to PID. To allow electrical measure-

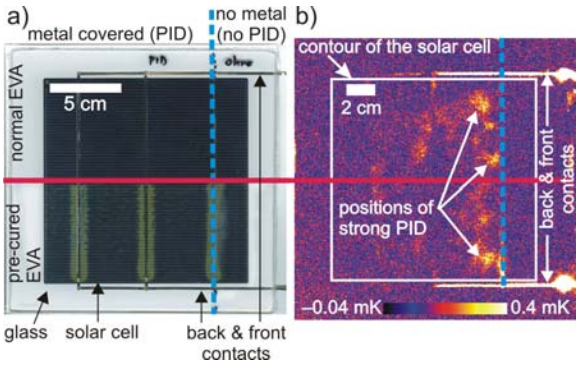


**Figure 1** (online colour at: www.pss-rapid.com) a) Photograph of the mini module. b) DLIT image taken at 0.3 V and 3 Hz lock-in frequency.

ments, the solar cell was soldered to commercially available contact ribbons. A one-cell mini module (Fig. 1a) has been prepared using soda lime glass, EVA on the front and back of the solar cell, and a typical back sheet. However, since elaborate investigations on the cell after the PID procedure were planned, it was necessary to disassemble the mini module later on without breaking the cell into undersized pieces. Furthermore it was necessary to avoid any residual EVA on the front side of the cell. For this purpose, half of the cell was covered with normal EVA whereas the other half was covered with pre-cured EVA foil prior to module lamination, as indicated in Fig. 1 by the solid red line. The larger part of the glass surface was homogeneously grounded using a metal foil, a smaller part was left uncovered, see the dotted blue line in Fig. 1.

PID has been generated by applying –600 V to the shorted cell contacts for 24 h at 85% relative humidity and 85 °C. During the degradation process, $R_p$ of the mini module has been recorded through cyclic current measurements at –0.5 V between the solar cell contacts. These measurements reveal a strong decrease of $R_p$ from 240 Ω to below 1 Ω within the first hour after initiating PID, which proved the degradation of the cell. After the PID test the outer appearance of the mini module has found to be unchanged.

Dark lock-in thermography (DLIT) investigation of the mini module presented in Fig. 1b revealed large area shunting in the region covered by the metal foil. There is no significant difference of shunt distribution between the region with pre-cured EVA and that with normal EVA. The area which was not covered by the metal foil, does not show any DLIT signal indicating that there was no PID in this part of the cell.

After sawing the glass into pieces, it was possible to prepare several 1 to 2 $cm^2$ sized solar cell pieces with a clean surface in the region with pre-cured EVA, both from degraded and unaffected regions of the mini module, i.e. right and left of the dotted blue line and below the red line, see Fig. 1. *I–V* curves of these samples show completely different behavior: The sample from the PID area has a linear *I–V* characteristic with a very small resistance of 1.4 Ω, whereas a sample from the non-PID area shows a typical rectifying characteristic of a p–n junction.

It is hard to perform normal EBIC on strongly shunted samples due to their low resistivity. However, images could be taken using a lock-in EBIC technique under the same conditions at a degraded and an unaffected sample and are presented in Fig. 2. The degraded sample shows very low lock-in EBIC signal between the grid fingers, whereas the non-degraded sample shows the typical signal due to carrier collection at the p–n junction, see Fig. 2a and 2b. The low lock-in EBIC signals in the PID sample are found to be point-like with diameters between 10 µm and 30 µm in this case. Some of these spots are indicated by arrows in Fig. 2a and in the higher magnified image in Fig. 2c. In a further step, a time-of-flight SIMS depth profile has been acquired at the red marked area in Fig. 2c. Positively charged secondary ions, sputtered from the topmost few-atom layers of the sample due to a scanning pulsed $Bi^+$-ion bombardment, were analyzed. Note, that the actual charge state in the sample, e.g. Na or $Na^+$, cannot be resolved. After each scan the surface is periodically eroded on a larger area with an intense (~200 nA) 1 keV $O_2^+$-ion beam. In this way a three-dimensional SIMS profile was obtained. Generally, a high $Na^+$ signal was observed in the nitride layer, but close to the Si surface the $Na^+$ signal showed locally small peaks. Figure 2d shows a map of the difference of the SIMS intensities $I_1$ and $I_2$ collected from 800 to 900 s and from 700 to 800 s after the beginning of the measurement, respectively. This corresponds to a depth close to the Si surface. This difference map improves the visibility of the $Na^+$ signals marked in Fig. 2d. The positions of the points of strongly decreased EBIC signal correspond very well with the position of increased $Na^+$ intensity measured by SIMS.

A model of the degradation mechanism will be proposed in the following. According to the results of the EBIC measurements the low $R_p$ after PID is caused by a

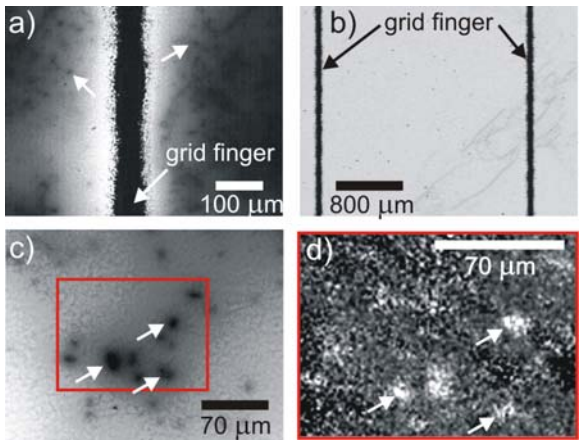


**Figure 2** (online colour at: www.pss-rapid.com) a) Lock-in EBIC image of the PID sample and b) lock-in EBIC image of the non-PID sample. c) Detailed lock-in EBIC image of the PID sample and d) corresponding SIMS-difference $Na^+$ map.

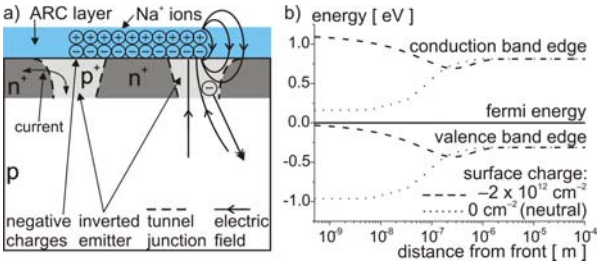


**Figure 3** (online colour at: www.pss-rapid.com) a) Solar cell cross section: Schematic of the proposed charge double layer leading to the shunt paths in the p–n junction. b) PC1D band diagrams for a solar cell without (dotted curve) and with (dashed curve) negative surface charge.

huge number of microscopic current paths through the emitter. Macroscopically, this appears to be a homogeneous ohmic shunt. At the shunt positions no emitter exists anymore, which is indicated by the point-like decreased EBIC signals there. Our hypothesis is that the $n^+$ emitter is inverted into a $p^+$ layer at these positions, and the shunting is due to a tunnelling current at the newly formed $p^+$–$n^+$ junction, see Fig. 3a. The question is how the inversion of the highly doped $n^+$ emitter can be explained?

Due to the high voltage in the sample between solar cell and glass surface, positive ions, e.g. sodium ions, migrate towards the ARC layer, leading to the observed leakage current [2, 4]. Positive ions in the vicinity of the Si surface are expected to increase the electron concentration in the emitter rather than inverting it. Furthermore, sodium is not known to act as shallow acceptor in Si [10], which could overcompensate the emitter.

In the proposed model it is assumed that at some positions in the ARC layer, the approaching positive charges attract or create a layer of negative charges between the layer of positive charges and the $n^+$ emitter, see also [8, 11], as shown in Fig. 3a. The nature of these negative charges is not clear yet. It is known that negative charges can be generated in silicon nitride layers on silicon by positive charges deposited on the nitride layers [11, 12]. It can be also speculated that, e.g., sodium compounds, $O^{2-}$ or $OH^-$ ions donated by a residual or native $SiO_2$ layer between the emitter and the ARC layer are involved [13].

The resulting electrical field of the charge double layer repels the emitter electrons. If the amount of charges and the resulting electrical field are large enough, the emitter might be even inverted to a $p^+$ conducting region. This explains the described tunnel junction leading to the observed low $R_p$ of the solar cell. The inversion is suspected to occur first underneath the edges of the charge double layer where the electrical field is largest.

To further motivate that a negative charge in front of the emitter may lead to an inversion of the $n^+$ emitter, the device simulation program PC1D [14] is used. Unfortunately, it was not possible to define a surface charge density $n_{sc}$ in the program which was high enough to show the inversion of a typical industrial $n^+$ emitter (emitter sheet resistance ~60 Ω/sq). If $n_{sc}$ exceeded $10^{13}$ $cm^{-2}$ significantly, the simulation did not converge. However, by increasing the emitter sheet resistance, it is possible to get an inversion of the entire emitter to a $p^+$-conducting region. Figure 3b shows the result of a typical simulation. This simulation included a p-type base doping of $1.51 \times 10^{14}$ $cm^{-3}$ and an emitter represented by two front n-type Gaussian diffusions with peak dopings of $5 \times 10^{16}$ $cm^{-3}$ and $1 \times 10^{16}$ $cm^{-3}$. These parameters still realize a typical kink-tail profile of the emitter and a normal shape of the band bending at the junction, just at lower doping concentration. The band diagram without any surface charge is shown by the dotted lines in Fig. 3b revealing a "normal" p–$n^+$ junction. By applying an $n_{sc}$ of $-2 \times 10^{12}$ $cm^{-2}$, the bands changed from a rectifying p–$n^+$ junction to flat band p–$p^+$ conditions as shown in Fig. 3b by the dashed lines. By varying the emitter sheet resistance, it was found that the value of $n_{sc}$ necessary to invert the emitter was approximately equal to the amount of electrons originally present in the emitter. It can be estimated from this finding that $n_{sc} \sim -10^{15}$ $cm^{-2}$ would be sufficient to invert a typical industrial emitter.

In conclusion, the microscopic structure of PID is found to consist of several micron-sized ohmic shunts. The positions of the shunts correlate with locally increased sodium concentration in the ARC layer of the cell. A model of a locally inverted emitter due to a charge double layer is proposed explaining the formation of the observed shunts causing PID.

**Acknowledgements** We gratefully acknowledge Q-Cells SE for providing the samples. The contribution of Fraunhofer CSP was financially supported by the BMBF project "FutureFab" (13N11446).

## References

[1] S. Pingel et al., in: Proceedings 35th IEEE PVSC, Honolulu, HI, USA, 2010, pp. 2817–2822.
[2] J. A. del Cueto et al., Prog. Photovolt., Res. Appl. **10**, 15 (2002).
[3] M. Schütze et al., in: Proceedings 26th EUPVSEC, Hamburg, Germany, 2011, pp. 3097–3102.
[4] P. Hacke et al., in: Proceedings 25th EUPVSEC, Valencia, Spain, 2010, pp. 3760–3765.
[5] M. Schütze et al., in: Proceedings 37th IEEE PVSC, Seattle, WA, USA, 2011, pp. 821–826.
[6] H. Nagel et al., in: Proceedings 26th EUPVSEC, Hamburg, Germany, 2011, pp. 3107–3112.
[7] S. Koch et al., in: Proceedings 26th EUPVSEC, Hamburg, Germany, 2011, pp. 1726–1731.
[8] V. Naumann et al., Energy Procedia (2012), in press.
[9] P. Hacke et al., in: Proceedings 37th IEEE PVSC, Seattle, WA, USA, 2011, pp. 814–820.
[10] J.-W. Chen et al., Annu. Rev. Mater. Sci. **10**, 157 (1980).
[11] H. Nagel et al., in: SOPHIA Workshop, Lugano, Switzerland, 2012.
[12] K. J. Weber et al., Appl. Phys. Lett. **94**, 063509 (2009).
[13] E. H. Snow et al., J. Appl. Phys. **36**, 1664 (1965).
[14] P. A. Basore, IEEE Trans. Electron Devices **37**, 337 (1990).